Porvali, Antti; Chernyaev, Alexander; Shukla, Sugam; Lundström, Mari

Lithium ion battery active material dissolution kinetics in Fe(II)/Fe(III) catalyzed Cu-H_2SO_4 leaching system

Published in:
Separation and Purification Technology

DOI:
10.1016/j.seppur.2019.116305

Published: 01/04/2020

Document Version
Publisher's PDF, also known as Version of record

Please cite the original version:
Porvali, A., Chernyaev, A., Shukla, S., & Lundström, M. (2020). Lithium ion battery active material dissolution kinetics in Fe(II)/Fe(III) catalyzed Cu-H_2SO_4 leaching system. *Separation and Purification Technology*, *236*, Article 116305. https://doi.org/10.1016/j.seppur.2019.116305

Separation and Purification Technology 236 (2020) 116305

Contents lists available at ScienceDirect

Separation and Purification Technology

journal homepage: www.elsevier.com/locate/seppur

Lithium ion battery active material dissolution kinetics in Fe(II)/Fe(III) catalyzed Cu-H_2SO_4 leaching system

Antti Porvali, Alexander Chernyaev, Sugam Shukla, Mari Lundström*

Aalto University, Department of Chemical and Metallurgical Engineering, Laboratory of Hydrometallurgy and Corrosion, Finland

ARTICLE INFO

Keywords:
Kinetics
Leaching
$LiCoO_2$
Iron reductant-oxidant

ABSTRACT

In mechanical recycling and separation of waste lithium-ion batteries (LIBs), Cu from electrode materials and Fe from battery casings may partially end up into the fine black mass fraction, rich in oxides such as $LiCoO_2$. Herein the kinetics of $LiCoO_2$-H_2SO_4-Fe-Cu- system was investigated by leaching studies in a 500 cm^3 glass reactor at $T = 30\,^{\circ}C$, with 2 M H_2SO_4 under $N_2(g)$ purging (0.5 dm^3/min). Design of experiments (DOE) was utilized as a supporting tool in investigation of the effect of copper ($Cu/2LiCoO_2 = 0.5–1.5$ mol/mol,) and iron ($Fe/LiCoO_2 = 0.01–0.11$ mol/mol) to the measured $LiCoO_2$ dissolution rate constants at initial phase of leaching (0–30 min) and at final phase of leaching (30–120 min). Analysis of variance showed that the kinetic rate constant models are statistically significant ($p = 0.002$ and $p < 0.000$, respectively), furthermore, the models describe real effects (coefficient of determination, $R^2 = 0.920$ for < 30 min model and $R^2 = 0.9895$ for > 30 min model). The results suggest that Cu is able to relinquish electrons to ferric ions, and the resulting ferrous ions mediate the transfer of electrons enabling reduction of $LiCoO_2$. A sufficient Co extraction (> 95%) was achieved with solution containing dissolved iron (1.06 g/L), along with 2.167 g of metallic Cu per 6.68 g of $LiCoO_2$ (1/1 mol ratio). It was calculated that the copper present in typical spent LIB cells is enough to satisfy this requirement. This decreases the chemical consumption as there is no need for external reductant.

1. Introduction

Secondary lithium-ion batteries (LIB) are increasingly being utilized in electric storage in various applications, from consumer electronics, to electric vehicles and stationary storage. This rapid growth highlights also the necessity for recycling of the end-of-life (EoL) batteries, as the batteries may contain a wide variety of metals such as Cu and Al in current collectors and Li, Co, Ni, Mn, Al in the active materials [1]. In addition there are polymeric separators, electrolyte salts (e.g. $LiPF_6$), binders as well as graphite from anode [2,3]. Furthermore, the way battery residing in a battery pack is utilized throughout its life may influence its properties [4], and hence, the recycling of the said batteries. Prior to metallurgical processing, the batteries are typically dismantled, discharged and crushed. Hydrometallurgical processing of battery waste may provide advantages over pyrometallurgical, namely by providing a possibility for a more complete recovery of elements, as no slags are generated from where certain elements, such as Li, may be difficult to recover [5]. Furthermore, it provides an opportunity to explore the recovery and reuse of graphite from anode [6]. In hydrometallurgical processing, the LIB waste, or the Co/Ni-rich fraction of the said waste, is firstly dissolved into the solution, after which both impurities (e.g. Fe, Al) as well as valuable metals (e.g. Co, Ni, Li) are recovered by dedicated solution purification, separation and product recovery steps of which there exists several examples [7–10].

Many different lixiviants, such as mineral acids and organic acids have been utilized in the hydrometallurgical recycling of LIBs [11]. However, in terms of industrial production, only few acids remain viable in terms of price and technology. One of the most often employed lixiviant is sulfuric acid (H_2SO_4). Sulfuric acid leaching has been often reported in the literature, and it remains as one of the most viable lixiviant due to its chemical stability and low cost. *Nan et al.* [12] were the first to report the leaching reaction of $LiCoO_2$ in sulfuric acid, and proposed the reaction to be occurring according to Eq. (1):

$$4LiCoO_2 + 6H_2SO_4 = 2Li_2SO_4(aq.) + 4CoSO_4(aq.) + O_2(g) + 6H_2O \qquad (\Delta G = -734.121\ \text{kJ}) \tag{1}$$

The $LiCoO_2$ (LCO) and the different types of $LiNMCO_2$ (NMC) batteries all rely on high electrode potentials. It is commonly known that in order to obtain excellent Co extractions, the active cathode materials present in lithium ion batteries (LIB) require a reductant during leaching due to the stability of the present higher-valence oxides [11].

---

* Corresponding author at: P.O. Box 12200, 00076 AALTO, Finland.
E-mail address: mari.lundstrom@aalto.fi (M. Lundström).

https://doi.org/10.1016/j.seppur.2019.116305
Received 9 September 2019; Received in revised form 26 October 2019; Accepted 7 November 2019

Ferreira et al. (2009) proposed that the reaction between $LiCoO_2$ and H_2SO_4 would stop due to formation of acid-resistant Co_3O_4, composed of trivalent and divalent cobalt, also emphasizing the need to use a reductant in battery recycling [13]. The subject of Co_3O_4 formation in hydrothermal treatment of $LiCoO_2$ has been also studied by *Fernández-Rodríguez et al.* (1988), who showed that at elevated temperature, delitihiated Li_xCoO_2 will transform to Co_3O_4 [14]. Several researchers have investigated the use of different reductants in sulfuric acid leaching of LIBs, these reductants including H_2O_2 [15], SO_3^{2-}/SO_5^{2-} from various sources [16], ascorbic acid [2], current collector scrap [17,18] and more. These reductants all have different standard reduction potentials to the point where some are usually referred to as oxidants. A strategy widely employed in contemporary research is the use of hydrogen peroxide (H_2O_2) (Eq. (2)) as a reductant (ranging in conc. from 1 to 10 vol% [11]) in the leaching of battery waste for the leaching of pure virgin cathode materials [13]:

$$4LiCoO_2 + 6H_2SO_4 + 2H_2O_2 = 2Li_2SO_4(aq.) + 4CoSO_4(aq.) + 2O_2(g) + 8H_2O \tag{2}$$

However, H_2O_2 has a controversial role as a reductant – in addition to $LiCoO_2$ reduction (reactions (8) and (12) in Table 1), it will act as an oxidant to the most of the other elements and compounds present in the battery waste (e.g. reactions (6) and (11)), and will therefore be simultaneously consumed by reactions that are unrelated to dissolution of active materials, such as $LiCoO_2$. Table 1 shows the reduction potentials in water for some of the half-cell reactions, relevant for the investigated system, which were obtained using the thermodynamic database of HSC 9.9 [19] at $T = 30\,^{\circ}C$.

In addition, H_2O_2 is readily decomposed catalytically through complex set of reactions involving radical formation by Fe^{2+} ion, a mixture known as a Fenton's reagent or Fenton's process, utilized extensively in wastewater treatment [20]. Haber-Weiss process, named after the persons who discovered the property, also utilizes this decomposition reaction [21]. Presence of dissolved Fe ions may therefore lead to autocatalytic losses of H_2O_2 during LIB waste treatment. Furthermore, rapid O_2 generation (Eqs. (1) and (2) caused by the reduction of the peroxide in (8)) during leaching may necessitate safety measures. A major advantage of H_2O_2 is that no additional impurities, such as sodium in case of Na_2SO_3, is added into the process. Regardless, based on all the above-mentioned facts, exploring alternatives for H_2O_2 is prudent.

1.1. *$LiCoO_2$ dissolution in presence of impurities*

Part of the complexity of understanding the leaching reactions occurring in the recycling of LIB waste is the heterogeneity of the mechanically processed raw materials. The LIB waste can contain traces of metallic Al, Cu and Fe as the batteries itself have these elements in current collectors (Al, Cu) and casing (Fe). Recent literature has shown that there are three viable strategies to handle Cu present in spent LIBs in mechano-hydrometallurgical way: avoid its dissolution in leaching [2], remove Cu foils in mechanical pre-treatment [22] or try to totally dissolve everything, recovering Cu hydrometallurgically later on in the process [8]. In battery waste, $LiCoO_2$ exists as a powder that is attached to an aluminum current collector as a slurry that incorporates an organic binder such as PVDF [1]. *Joulié et al.* studied the use of the current collectors as a reducing agents [17]. They showed that Al and Cu both separately enhanced the dissolution of $LiCoO_2$. In the case of Al, they determined that the reducing power most likely comes from the hydrogen gas evolution (i.e. acid reduced by electrons released in Al oxidation) and subsequent oxidation of $H_2(g)$, shown in Eqs. (13) and (14):

Table 1

Standard reduction potentials of system components, calculated at T = 30 °C.

Half Cell Reaction	E_0 (V vs. SHE)	Reaction no.
$Fe^{2+} + 2e^- = Fe(s)$	−0.408	(3)
$2H^+ + 2e^- = H_2(g)$	0	(4)
$Cu^{2+} + e^- = Cu^+$	0.160	(5)
$Cu^{2+} + 2e^- = Cu(s)$	0.337	(6)
$Cu^+ + e^- = Cu(s)$	0.515	(7)
$O_2(g) + 2H^+ + 2e^- = H_2O_2(l)$	0.619	(8)
$Fe^{3+} + e^- = Fe^{2+}$	0.644	(9)
$O_2(g) + 4e^- + 4H^+ = 2H_2O$	1.225	(10)
$H_2O_2(l) + 2H^+ + 2e^- = 2H_2O$	1.832	(11)
$LiCoO_2(s) + 4H^+ + e\text{-} = Li^+ + Co^{2+} + 2H_2O$	2.152	(12)

$$2Al + 3H_2SO_4 = Al_2(SO_4)_3(aq.) + 3H_2(g) \quad (\Delta G = -1131.668\ \text{kJ}) \tag{13}$$

$$2LiCoO_2 + 2H_2(g) + H_2SO_4 = Li_2SO_4(aq.) + 2CoSO_4(aq.) + 4H_2O \quad (\Delta G = -603.386\ \text{kJ}) \tag{14}$$

It is also possible that Al foils cause galvanic corrosion, however this would require the $LiCoO_2$ to be in electrical contact with the Al reagents.

Cu can be oxidized by atmospheric oxygen in acidic solutions (Reactions (6) and (10)):

$$2Cu + 4H^+ + O_2(g) = 2Cu^{2+} + 2H_2O \quad (\Delta G = -342.566\ \text{kJ}) \tag{15}$$

Thermodynamically, Cu can also dissolve via galvanic interaction, as it contains the potential to reduce $LiCoO_2$, reactions (6) and (12). However, this would necessitate an electrical contact between metallic Cu and $LiCoO_2$ and there is uncertainty whether this occurs. Galvanic interaction, shown in Eq. (16) will be investigated in the present study:

$$2LiCoO_2 + Cu + 4H^+ = 2Li^+ + Cu^{2+} + 2Co^{2+} + 2H_2O \quad (\Delta G = -350.017\ \text{kJ}) \tag{16}$$

Also, it must be noted that without the presence of stabilizing ligands such as ammonia or chloride, Cu^+ is an unstable ion in aqueous sulfate media, therefore Cu^{2+} cannot oxidize Fe^{2+} in sulfate system, as shown in Eq. (17):

$$Cu^{2+} + Fe^{2+} = Cu^+ + Fe^{3+} \quad (\Delta G = 46.637\ \text{kJ}) \tag{17}$$

Ferrous ions can also be oxidized to ferric ions by presence of a stronger oxidant, such as dissolved $O_2(g)$, reactions (9) and (10) combined, shown in Eq. (18):

$$4Fe^{2+} + O_2(g) + 4H^+ = 4Fe^{3+} + 2H_2O \quad (\Delta G = -224.400\ \text{kJ}) \tag{18}$$

In industrial recycling processes, good mechanical separation of Cu and Al foils and Fe casings from the active material rich fraction can be achieved [3,23]. However, depending on the thoroughness of the mechanical separation, Cu, Fe and Al can find their way to the black mass fraction in significant quantities ($Fe = 0.72$ wt%, $Cu = 3.02$ wt%) [3]. In these cases, it is essential to better understand the interactions that these solids and their dissolved ions may pose in the leaching system. Casas et al. have also studied the dissolution of copper by ferric ions in sulfuric acid, however the conditions are dissimilar to that used in battery recycling [24,25].

$$Cu + 2Fe^{3+} = Cu^{2+} + 2Fe^{2+} \quad (\Delta G = -59.083\ \text{kJ}) \tag{19}$$

It has been shown by *Peng et al.* (2019) that the dissolution of $LiCoO_2$ in real waste can proceed with addition of metallic Cu, originating from current collectors, into solution that contains dissolved ferrous ions, as shown in Eq. (20) (Reactions (12) and (9)) and Eq. (19) (Reactions (6) and (9) [18]:

$$Fe^{2+} + LiCoO_2 + 4H^+ = Li^+ + Co^{2+} + Fe^{3+} + 2H_2O \quad (\Delta G = -145.467 \ \text{kJ}) \tag{20}$$

There is also evidence for this reaction in the work of *Mishra et al.*, however it was not recognized as such in the study [26]. In present work, it is suggested that the reactions (19) and (20) be combined to yield the total catalytic reaction (21):

$$2LiCoO_2 + Cu + 8H^+ \xrightarrow{Fe(II)/Fe(III)} 2Li^+ + 2Co^{2+} + 4H_2O + Cu^{2+} \tag{21}$$

It would therefore appear that a H_2O_2 free leaching system could potentially utilize dissolved iron as well as elemental Cu present in the current collectors for the reduction of $LiCoO_2$. Iron ions act as a redox catalyst, mediating the dissolution of both Cu and $LiCoO_2$. As the *Peng et al.* (2019) study did not investigate the mechanism of reactions (19–21) at a deeper level, and as the effect of impurities associated with Cu and Al foils were not controlled, more in-depth understanding about this phenomenon is therefore required on how the Fe and Cu impurities may affect the dissolution of battery active materials in their hydrometallurgical recycling, and whether therefore they could be utilized as a primary reductant instead of H_2O_2. As the driving force is not that large for the reaction (19) and in addition, the total reaction (21) may potentially be slow as several adsorption, desorption, diffusion and mass transfer events are required for electrons to be carried from Cu to $LiCoO_2$ by iron ions, and it is uncertain that what is the lowest Fe concentration where the proposed reaction (21) can occur. Furthermore, the atmospheric oxygen may prove problematic as it can cause Cu dissolution according to reaction (15). Because of all these factors, kinetics of the leaching system proposed in the hypothesized reaction (21) were investigated in the current study with synthetic reagents. A novel way of utilizing design of experiments (DOE) in supporting the analysis of leaching kinetics is shown, which demonstrates how the rigorousness of the results can be evaluated more thoroughly by applying the principles of DOE along with more traditional kinetic experiments and their methods of evaluation. In the present study, the investigation was limited to Cu, Fe and $LiCoO_2$, excluding Al.

2. Materials & methods

2.1. Kinetic experiments

The experiments were performed in a 500 cm^3 jacketed glass reactor made of borosilicate glass (Lasilaite, Finland). The reactor was heated to target temperature by the attached water bath and circulating thermostat (Lauda A100, Germany). A condenser was attached to the reactor, and the reactor was sealed with glass stoppers, silicon band and steel clamp. Prior every experiment, the solution media was prepared by measuring 200 cm^3 of 4 M sulfuric acid which was diluted to 2 M during the leaching medium preparation. Total volume of 400 cm^3 of the lixiviant was used. The 4 M sulfuric acid was prepared from concentrated stock (H_2SO_4, 95–97%, VWR Chemicals). The concentration of the prepared 4 M H_2SO_4 was confirmed with acid-base titration (Phenolphtalein, 1%, FF-Chemicals, Indicator; 2.0 N NaOH, standardized solution, Alfa Aesar). Ferrous sulfate ($FeSO_4{\cdot}7H_2O$, > 99% ACS Grade, Alfa Aesar) was added in the lixiviant preparation stage, and was included in the total volume. In order to avoid the presence of atmospheric O_2 in the solution, a constant $N_2(g)$ purging (0.5 dm^3/min) was applied via Teflon tubing throughout all the experiments by using a rotameter (LH-ZC50-HR, Kytölä, Finland), This was done to avoid reactions (5) and (8). Gas was always injected for at least 10 min prior the addition of lithium cobalt oxide ($LiCoO_2$, > 99.5%, Alfa Aesar). All experiments used 6.68 g of $LiCoO_2$. Copper powder (< 425 µm Cu, 99.5%, Alfa Aesar) was also added only after 10 min of purging, and further 10 min was waited before $LiCoO_2$ addition.

Sampling was done with a glass pipette, retrieving ca. 3–4 cm^3 of sample. Sampling intervals were 5, 10, 15, 30, 60 and 120 min. The sample was syringe filtered with 0.45 µm polyethylene sulfone (PES) membranes, and stored for atomic absorption spectroscopy (AAS, Thermo Fisher, ICE 3000, USA) analysis. Co, Cu and Fe were analyzed from every sample. The collected leach residues were filtered with Whatman grade 50 filter papers with a vacuum filtration assembly. The residues were dried in an oven at 60 °C overnight. Select samples based on the dissolution results were analyzed with x-ray diffraction (XRD, X'Pert Pro MPD Powder, USA, equipped with PIXcel1D detector, Co Kα source operated at 40 kV, 40 mA, along with Fe beta filter and no monochromator), and scanning electron microscope (SEM, Tescan Mira3, Czech Republic) equipped with energy-dispersive X-ray spectroscopy (EDS, ThermoFisher Scientific, Ultradry EDS Detector, USA), where respectively needed. The collected filtrate was let to cool down, after which its volume was measured to ascertain the final volume with graduated cylinder.

Table 2
The experiments and their parameter levels that were utilized in this study. $LiCoO_2$ mass in brackets indicate the value used in calculations only.

Experiments Code	H_2SO_4 (M)	T (°C)	$FeSO_4{\cdot}7H_2O/LiCoO_2$ (mol/mol)	$Cu/2LiCoO_2$ (mol/mol)	$LiCoO_2$ (g)
A1	2	30	0	1.5	0 (6.68)
A2	2	30	0	0	6.68
A3	2	30	0.5	0	6.68
A4	2	30	1	0	6.68
A5	2	30	1.5	0	6.68
A6	2	30	0.01	1.5	6.68
A7	2	30	0.01	0.5	6.68
A8	2	30	0.11	1.5	6.68
A9	2	30	0.055	0.5	6.68
A10	2	30	0.055	1	6.68
A11	2	30	0.055	1.5	6.68
A12	2	30	0.11	0.5	6.68
A13	2	30	0.055	1	6.68
A14	2	30	0.11	1	6.68
A15	2	30	0.01	1	6.68
A16	2	30	0.055	1	6.68
A17	2	30	0	1.5	6.68
A18	2	30	0	1.5	6.68

Experiments A2–A5, shown in Table 2, were done to ascertain whether ferrous ions are capable of dissolving $LiCoO_2$ on its own, whether an excess is required and whether the reaction rate is measurable. Experiments A1, A17 and A18 were done in order to ascertain the effect of $LiCoO_2$ can have on Cu dissolution. In A18, $LiCoO_2$ and H_2SO_4 was let to react for 1 h, after which Cu was added. The result (Cu extraction and Co concentration) of A18 was then compared to A1 and A17. Experiments measuring the effect of Cu and Fe on reaction rate, A6–A16, were planned by utilizing response surface methodology (RSM), a group of tools belonging to DOE [27]. This tool provides several benefits to the analysis of results. Firstly, it maximizes the obtained knowledge about the system per number of experiment, yielding a regression model for interpolative prediction; secondly, it utilizes statistics, enabling the user to easily identify the outliers and problems in the reliability of the data; thirdly, it provides unconfounded information about the behavior of the investigated parameters: linear, interaction and binomial effects are observed separately. A central composite design (CCD) was utilized with three center point replicates and Minitab software was used in the analysis of CCD [28]. Ferrous sulfate and copper metal were the investigated factors, and the responses recorded were reaction rate constant by cubic rate law at 0–30 min and at 30–120 min. In the CCD, as a star point α = 1 was chosen, hence the response surface design can be called face-centered central composite (CCF), and was identical to 2^3 full factorial design. This design gives worse curvature detection than circumscribed central composite design but is easier to implement within the desired parameter constraints. In the design, three replicates of the center point was obtained for the estimation of lack-of-fit.

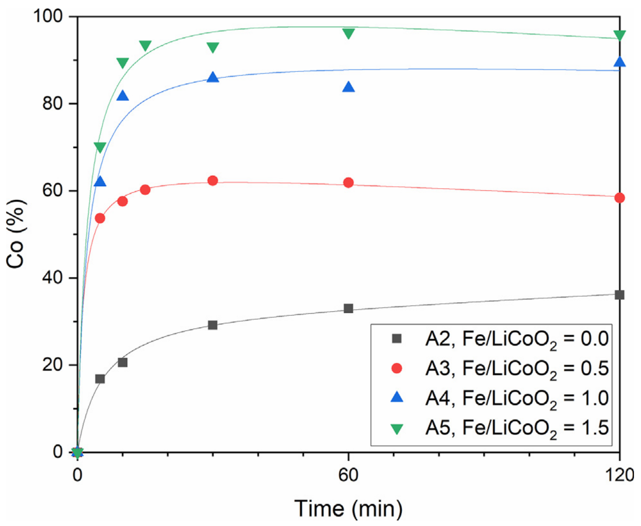

Fig. 1. Results of experiments A2-5, depicting the effect of ferrous ions on Co extraction from $LiCoO_2$.

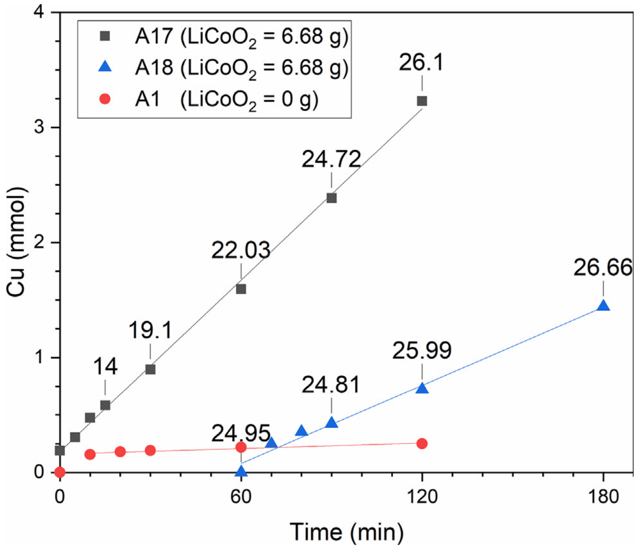

Fig. 2. The effect of $LiCoO_2$ on dissolution of Cu. A1 had no $LiCoO_2$. In A18, Cu was added only after 1 h of reactions was allowed for $LiCoO_2$. The dissolved Co (mmol) at select points is shown above the data points of A17 and A18. T = 30 °C, $[H_2SO_4]$ = 2 M.

3. Results & discussion

3.1. Effect of individual impurities

In this section the individual effect of dissolved Fe and metallic Cu on dissolution of $LiCoO_2$ in sulfuric acid was investigated. We show that Fe(II) will strongly influence the dissolution of $LiCoO_2$, and that presence of $LiCoO_2$ influences the dissolution of Cu.

Firstly, the effect of ferrous ions were investigated independently, Fig. 1. It was found out that in the absence of iron, the total Co extraction was 37%. Opposite to this, the presence of ferrous sulfate was shown to enhance $LiCoO_2$ leaching substantially - stoichiometric quantity resulted in 90% Co extraction (A4), and with 1.5 times the stoichiometric excess a nearly complete dissolution of Co could be ensured (96%, A5). The $LiCoO_2$ dissolution reaction was shown to be very rapid in presence of ferrous ions, and already at 5 min extractions of 53%, 62% and 70% were achieved (A3-5). The results suggest that reaction (19) occurs between Fe(II) and $LiCoO_2$ and that it is unlikely that this step would be the rate limiting step in dissolution of $LiCoO_2$ in Cu-Fe-H_2SO_4 system in the presence of sufficient quantity of dissolved Fe(II). However, it remains unseen yet as to what the lower limit is, and will be explored in present study.

The dissolution of Cu in the absence and presence of $LiCoO_2$ was also investigated, Fig. 2. It was shown that the dissolution of metallic Cu is enhanced in presence of $LiCoO_2$, however, the extraction of Co i.e. reductive leaching of $LiCoO_2$ was not simultaneously improved. If the dissolution of Co were by galvanic interactions alone (reactions (6), (12) and (16)), one should see dissolution of 2 mol of Co per 1 mol of Cu which is not evident here. This is contrary to result of *Joulié et al.* who successfully utilized Cu foils in dissolving Li-NMC ($Li_{1.043}Ni_{0.333}Mn_{0.296}Co_{0.328}O_2$) active materials through galvanic interactions [17]. Therefore, the reaction mechanism with $LiCoO_2$ and Cu in sulfuric acid vs. NMC and Cu in sulfuric acid must be different, and may be related to combination of structural and chemical differences caused by replacement of some of the Co atoms with Ni and Mn in the structure of NMC cathode material. It has been shown by *Billy et al.* that NMC dissolution proceeds through delithiation, followed up by structural changes and formation of metastable phases [29]. This is different from LCO, where presence of Co_3O_4 has been reported due to structural reorganization. It is possible that some of the dissolution of Cu and Co in the present study may still be due to the galvanic interactions, however the effect is not pronounced enough to be clearly detected, Fig. 2. It can be seen that Cu dissolves faster when added immediately alongside with $LiCoO_2$ (A17), unlike in A18 where Cu was added only after 1 h of leaching time. However, in both cases the final Co concentration is practically the same (3945 mg/L in A17, 4028 mg/L in A18, 3725 mg/L in A2). Therefore, it can be concluded that Cu is not enhancing Co extraction in the studied environment, but the system must have a different oxidant enhancing Cu dissolution in presence of $LiCoO_2$. This is suggested to be indicative of reaction (1) producing $O_2(g)$ which would in turn oxidize metallic Cu according to Eq. (5).

From LIB recycling process point of view, using ferrous iron alone as a reductant is counterproductive, due to high Fe concentrations accumulating into the PLS and therefore causing burden for the following solution purification steps. In the current study the Fe concentrations used in the ferrous leaching experiments were 9.62 g/L of Fe (i.e. stoichiometric ratio of 1:1 in A4), and 14.43 g/L (i.e. stoichiometric ratio of 1:1.5 in A5). Therefore, the experiments utilizing Fe as a catalyst (reducing agent for $LiCoO_2$, reactions (9) vs. (12) and Cu as the reducing agent for Fe (reducing Fe(III) to (FeII), reactions (6) vs (9)), were performed according to RSM matrix (A6-A16). Extractions in

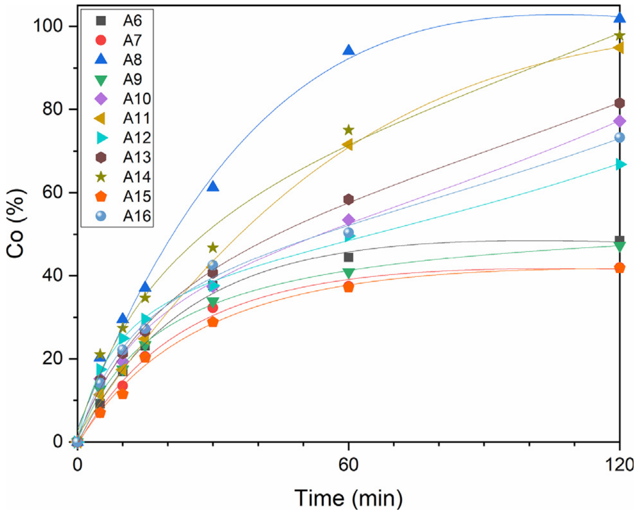

Fig. 3. The leaching yields of Co under varying Fe (Fe/$LiCoO_2$ = 0.01–0.11 mol/mol) and Cu (Cu/2$LiCoO_2$ = 0.5–1.5 mol/mol) parameters.

Fig. 3 show that total Co dissolution was achieved by having excess Cu (1.5 times) in the feed (A8, *Cu/2LiCoO$_2$* = 1.5, *Fe/LiCoO$_2$* = 0.11 (mol/mol)). It is evident that the LiCoO$_2$ dissolution kinetics is slower in experiments shown in Fig. 3 compared to Fig. 2. This highlights that the rate-limiting step in LiCoO$_2$ dissolution is dependent on the reactions between Fe and Cu rather than between Fe and LiCoO$_2$. Also, stoichiometric quantity of Cu was found to be enough to reach a nearly complete Co dissolution in two cases (A11, A14, *Fe/LiCoO$_2$* = 0.055 and 0.11 mol/mol, respectively). This can be explained by the initially available ferrous ions that help to dissolve LiCoO$_2$ according to reaction (20), along with the reaction between LiCoO$_2$ and sulfuric acid shown in A1 and A2. The varying amount of $FeSO_4{\cdot}7H_2O$ also explains the difference between the amount of Co dissolved. Compared to A3-A5, the amount of Fe utilized in experiments A6-A16 is small (0.01–0.11 Fe/LiCoO$_2$ (mol/mol)). Fig. 1 suggests that in the presence of ferrous ions alone, (with *Fe/LiCoO$_2$* = 0.5, most of the Fe(II) had already reacted by 5-minute mark (Fig. 1).

3.2. Reaction rates in LiCoO$_2$-Cu-Fe-H$_2$SO$_4$ system

In this section, the reaction rates for the dissolution of LiCoO$_2$ was measured in the catalytic dissolution system composed of metallic Cu, dissolved Fe and sulfuric acid. Limits of the dissolution system was investigated.

Reaction rates were investigated by applying shrinking core model with assumption of the leaching system being reaction controlled. Cubic rate law, shown in Eq. (22), was applied in the fitting of data [30]:

$$1-(1-x)^{\frac{1}{3}}=k_c{\cdot}t \tag{22}$$

where k_c is the reaction rate (min^{-1}), t is time (min) and x is the dissolved fraction (0–1). Most of the experimental series follow the cubic rate law well, with coefficient of determination (r^2) generally being in the range of 0.98–0.99, as shown in Fig. 4. However, the series A6, A7 and A9 did not follow the cubic rate law over the course of two hours. Regardless, when considering the first four samplings (first 30 min of the leaching), all the DOE experiments (A6–A16) follow the cubic rate law, Fig. 4. All linear fitted models exhibited $p < 0.05$, with r^2 being in range of 0.95–0.99. Fastest reaction rate at $t < 30$ min was observed with A8 (*Cu/2LiCoO$_2$* = 1.5, *Fe/LiCoO$_2$* = 0.11 (mol/mol)), while the slowest was A12 (*Cu/2LiCoO$_2$* = 0.5, *Fe/LiCoO$_2$* = 0.11 (mol/mol)). The difference in the reaction rates between the series that provided bad (Fig. 4B) and good (Fig. 4A) final extractions of Co is not great, yet – in fact, A12 had slower reaction rate than in A6, A7, A9 and A15.

The LiCoO$_2$ dissolution rate after 30 min was also plotted, Fig. 5A. Again, $p < 0.05$ was obtained, except for A16, which had p = 0.083. r^2 ranged from 0.98 to 0.99999, indicating a good fit. However, no good fit was obtained for the data presented in Fig. 5B. This is due to the fact that dissolution mechanism that is prevalent in the other cases has ceased to function, and LiCoO$_2$ dissolution was not any more controlled according to cubic rate law. In fact, in terms of Co extraction, dissolution had nearly ceased altogether in these experiments, as was shown in Fig. 1A. The fitted lines (A6, A7, A9 and A15) had $p > 0.1$ and r^2 ranged from 0.89 to 0.96. Several different kinetic models were tried, but none provided satisfactory results for these experiments between 30 and 120 min. Fastest reaction rate was again observed with A8 (*Cu/2LiCoO$_2$* = 1.5, *Fe/LiCoO$_2$* = 0.11 (mol/mol)). The reaction was slightly faster than in the initial stages ($7.89{\cdot}10^{-3}$ vs. $11{\cdot}10^{-3}$/min). Compared to reaction rates shown in Fig. 4B, reaction rates in Fig. 5B have decreased significantly and are now less than 0.001 min^{-1}.

3.3. Reaction rate analysis with design of experiments

In this section, the design of experiments was utilized in analyzing the reaction rates and the relation of their change as a function of *Cu/2LiCoO$_2$* (mol/mol) and *Fe/LiCoO$_2$* (mol/mol) content in the leaching system. This generates information about the change of the reaction rate, all the while providing a way to test the rigorousness of the results. Furthermore, it allows for creation of a binomial regression model for predicting the reaction rate constant within the investigated parameter ranges.

The reaction rate constants were used in creating two regression models, one for < 30 min (Model 1) and one for > 30 min (Model 2). The reaction rate constants that were used to fit the models are presented in Fig. 4 and 5. Initially, all terms were considered, including the linear terms *[Cu]*, *[Fe]*, their 2-way interaction term *[Fe·Cu]* and binomial terms *[Cu]*^{2} and *[Fe]*^{2}. Backward elimination was utilized in removing statistically insignificant terms at confidence level of 90% ($p < 0.1$). Initially, it was seen that the term *[Fe]*^{2} is statistically insignificant in both models (p = 0.180 and p = 0.567 in Model 1 and Model 2, respectively), and was thus removed. It can be therefore concluded that at the investigated parameter levels the reaction is not second-order in respect of Fe, but first order as *[Fe]* alone was statistically significant with confidence level > 99%. After removing the least significant parameter *[Fe]*^{2}, the model was refitted and *[Cu]*^{2} was inspected. It was decided that [Cu]^2 will be included in the models as the p = 0.102 and p = 0.088 in Model 1 and Model 2, respectively.

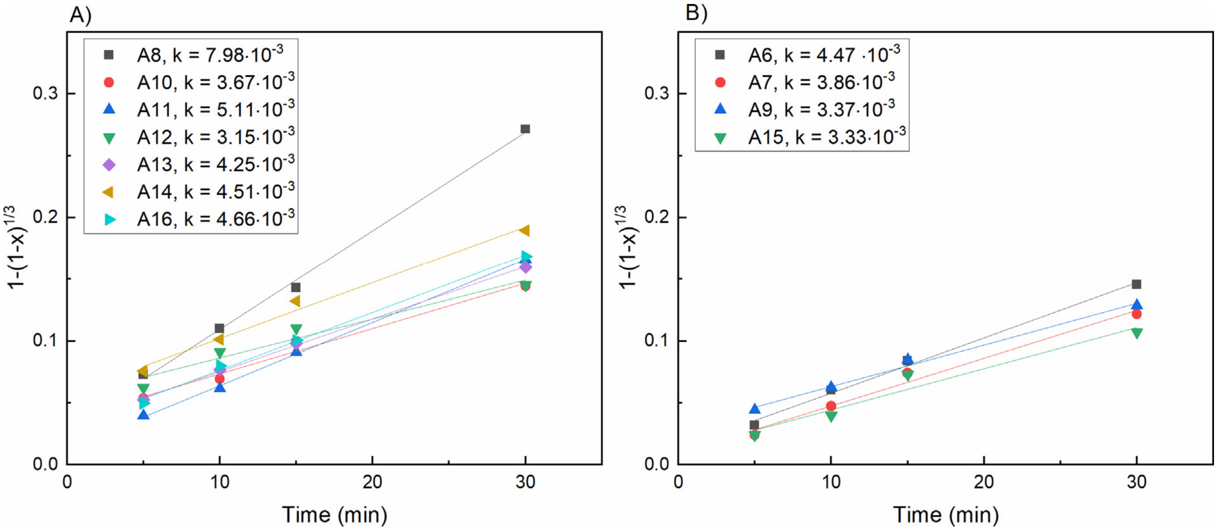

Fig. 4. (A) Reaction rate according to first 30 min, fitted to cubic rate law. Samples that exhibited significant decrease of reaction kinetics past 30 min are differentiated in (B).

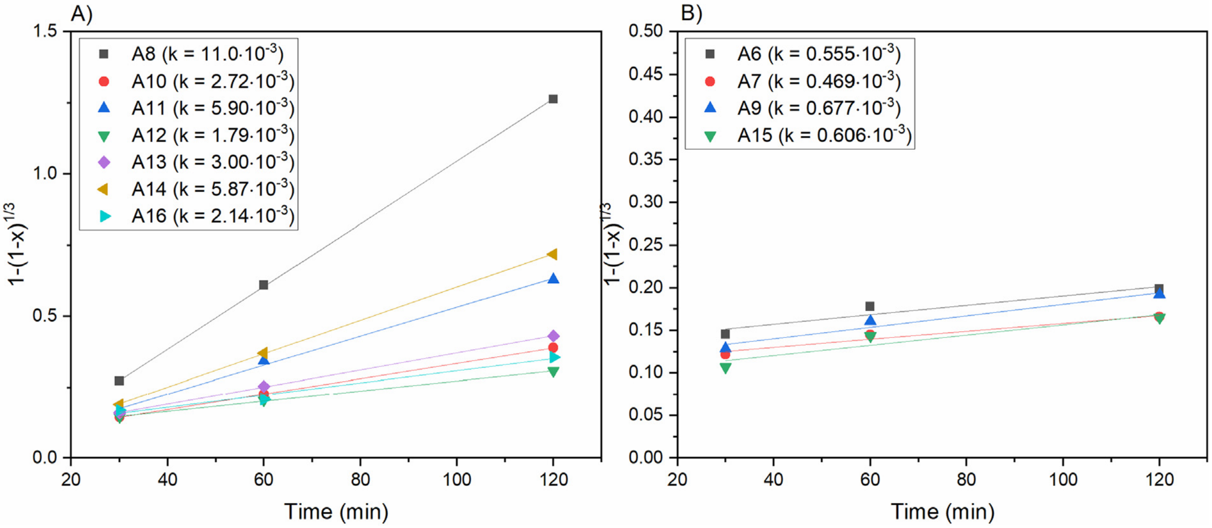

Fig. 5. (A) and (B): Reaction rates according to the last 120 min, fitted to cubic rate law. Samples that exhibited significant slowing of reaction kinetics past 30 min are differentiated in (B).

Table 3
ANOVA table for Model 1, k values for < 30 min.

Source	DF	Adj SS	Adj MS	F-Value	P-Value
Model	4	0.000017	0.000004	17.25	0.002
Linear	2	0.000011	0.000006	23.37	0.001
Fe	1	0.000003	0.000003	10.99	0.016
Cu	1	0.000009	0.000009	35.76	0.001
Square	1	0.000001	0.000001	3.72	0.102
Cu*Cu	1	0.000001	0.000001	3.72	0.102
2-Way Interaction	1	0.000004	0.000004	18.53	0.005
Fe*Cu	1	0.000004	0.000004	18.53	0.005
Error	6	0.000001	0		
Lack-of-Fit	4	0.000001	0	0.96	0.569
Pure Error	2	0	0		
Total	10	0.000018			

Table 4
ANOVA table for Model 2, k values for > 30 min.

Source	DF	Adj SS	Adj MS	F-Value	P-Value
Model	4	0.000105	0.000026	141.03	0
Linear	2	0.000083	0.000042	224.11	0
Fe	1	0.000048	0.000048	259.56	0
Cu	1	0.000035	0.000035	188.66	0
Square	1	0.000001	0.000001	4.13	0.088
Cu*Cu	1	0.000001	0.000001	4.13	0.088
2-Way Interaction	1	0.000021	0.000021	111.76	0
Fe*Cu	1	0.000021	0.000021	111.76	0
Error	6	0.000001	0		
Lack-of-Fit	4	0.000001	0	0.95	0.57
Pure Error	2	0	0		
Total	10	0.000106			

Based on criterion of confidence level of 90%, *[Cu]*^{2} could also be eliminated from the Model 1, but it is vital to interpret the results in terms of uncertainty caused by other reactions in the initial 30 min. It is likely that the same mechanisms are at work in both models. The final analysis of variance (ANOVA) tables are presented in Table 4 and Table 3. As can be seen in the Table 4 and Table 3, neither model has lack-of-fit: therefore the null hypothesis “There is lack of fit” can be rejected due to the fact that $p > 0.1$ ($p = 0.569$ and $p = 0.57$ for Model 1 and Model 2, respectively).

The model summaries along with the coefficients of determination (R^2) for each model are shown in Table 5. The Model 2 (> 30 min) for reaction rate constants is excellent, as only 1.05% of the model is explained by noise, and the predictive power of the model remains good even when individual data points are removed, model refitted and the removed data point is compared to the refitted model (R^2 (pred)). However, there is more noise in Model 1. This can be due to competing side-reactions according to Eqs. (1) and (5, 9–11). These factors may help to explain why 8% of the effects observed in Model 1 are attributable to noise. The effect of *[Cu]* and *[Cu]*^{2} is a decade weaker than the effect of *[Fe]* and 2-way interaction term *[Fe·Cu]*. Therefore, iron and the combination of iron and copper can be concluded to have the largest effect on the $LiCoO_2$ dissolution reaction rate. Both *[Fe]* and *[Cu]* alone negatively affect the reaction rate, however the interaction effect is much stronger than either combined. The negative effect of *[Fe]* can be interpreted based on results of Fig. 1: rapid reaction with ferrous iron resulted in slow leaching kinetics over time, than compared when there is no ferrous iron at all. The negative effect of Cu is also evident in Fig. 2. It is curious that Cu has a non-linear response, which in fact suggests that there may be several dissolution pathways of $LiCoO_2$ which are affected by the presence of Cu. This conclusion is supported by the results in Fig. 2. In the following section the possible reasons for the reaction mechanisms are explored by characterization of leach residues, and by analyzing the dissolved Fe and Cu contents. The uncodified models for reaction rate constants are presented in Eqs. (23) and (24).

It can be concluded that DOE, is a useful tool in applying additional rigor to analysis of kinetics of reactions. The resulting contour plot predicting the reaction rate constant for the 30–120 min of the dissolution (Model 2) is presented below, Fig. 6A. The contour plot demonstrates the interaction of *[Fe·Cu]* as non-vertical and non-horizontal lines, and the binomial effect of *[Cu]*^{2} is the cause for the curvature in lines. The plot again demonstrates if there were galvanic corrosion between $LiCoO_2$ and Cu, the effect is very small as k_c values do not react well to the increase of Cu when Fe amount is low. In Fig. 6B, the effect of noise is apparent by the presence of saddle-point. Results below k_c line 3.625 should be treated with skepticism.

3.4. Reaction mechanism

In this section, the quantities of Fe and Cu in the solution was

Table 5

Model summaries, showing model standard error of regression (S), coefficient of determination (R^2), number adjusted R^2 and the predicted R^2. The regression models are expressed as uncodified equations.

Model Summary	S	R^2	R^2(adj)	R^2(pred)
Model 2 (> 30 min)	0.000432	98.95%	98.25%	96.73%
$k_c = 0.00222 - 0.03447 \cdot Fe - 0.00489 \cdot Cu + 0.00213 \cdot Cu \cdot Cu + 0.09124 \cdot Fe \cdot Cu$#(23)				
Model 1 (< 30 min)	0.00049	92.00%	86.67%	62.14%
$k_c = 0.00572 - 0.0289 \cdot Fe - 0.00472 \cdot Cu + 0.00229 \cdot Cu \cdot Cu + 0.04220 \cdot Fe \cdot Cu$#(24)				

investigated. First, Fe levels are inspected for any changes that occurred during leaching. Second, the dissolution rates of Cu and Co are compared in order to see whether the proposed reaction mechanism is valid.

The reason for the decrease in the dissolution rate, along with the reason for binomial Cu response was investigated. Experiments A6 and A7 both had low amount of Fe ($Fe/LiCoO_2 = 0.01$ mol/mol), whereas the experiment A9 had the center quantity ($Fe/LiCoO_2 = 0.055$ mol/mol) of Fe and low quantity of Cu ($Cu/2LiCoO_2 = 0.5$ mol/mol). Solution samples A6, A7, A9 and A15 were analyzed for Fe contents as a function of time, Table 6. The samples with low Co extraction efficiency indicate gradual decrease in Fe contents. In both in A7 and A9 the decrease in Fe content is 6%, from 5 min to 120 min. Regardless, significant quantities of Fe yet remained in each solution sample of every series: the loss of the catalyst Fe could not be the reason for poor kinetics in A6, A7, A9 nor in A15.

Molar quantities of dissolved copper and cobalt were then compared. According to reaction (21), one mol of Cu may react with two mols of Co, assuming no dissolution due to external factors, such as dissolved oxygen, nor other unexpected reactions. The results are presented in Fig. 7, which shows how dissolved Co^{2+}/Cu^{2+} ratio of Exp. A8, A11 and A14 converges towards the ratio of 2. These experiments had the best Co extraction efficiencies (101.8%, 94.9% and 97.8%, respectively), and this is reflected on dissolved Cu. However, even though the dissolved mol ratio of $Co^{2+}/Cu^{2+} = 2/1$ supports the reaction presented in reaction (21), it is not immediately obvious that all the Cu is consumed by the said reaction. This was seen in the Fig. 1B as well, as Cu was dissolved due to external reasons. This argument is supported by experiment A8, which had a stoichiometric excess of Cu ($Cu/2LiCoO_2 = 1.5$), resulting in molar ratio of dissolved Cu/Co = 1.84. The experiments where Co did not dissolve well (A6, A7 and A15), it can be observed that the ratio initially increases, signifying that the dissolution kinetics of Cu is slower compared to that of Co. It is known from experiments A2 that sulfuric acid alone may dissolve *ca.* 37% of the Co present. This increase that can be observed in A6, A7 and A15, and is most likely due to the lack of catalyst Fe in the solution, as all three had low level of Fe present. Therefore the increase is suggested to be due to the dissolution of Co by H_2SO_4 alone, as shown in results of A2 (Fig. 1). However, again, the lack of Fe does not explain the poor dissolution kinetics of $LiCoO_2$, as A9 ($Fe/LiCoO_2 = 0.55$, $Cu/2LiCoO_2 = 0.5$, mol/mol) provided also a poor extraction and rate of reactions. The assumption is that the reason may be related to an insufficient mass transfer and reaction site opportunity, facilitated by the low reaction kinetics at $T = 30$ °C.

Subsequently, SEM-EDX and XRD were utilized in the analysis of leach residues. In analysis of results of A6-A16, select samples were inspected with SEM (A5, A6, A9, A10). The change in the morphology of the used copper powder was also observed, Fig. 8. The metallic copper has dissolved most strongly along its grain boundaries (bright phase), as can be seen from the cracks on the surface. It would also appear that some cobalt oxide (dark phase) has become lodged into the more dissolved areas of the copper particle, reducing the available surface area for the reactions. It is postulated that the mechanism by which Co is integrated to copper particle is not electrochemical in nature, but physical as clear grain boundaries can be seen between lighter and darker areas. Furthermore, EDX indicates that the areas containing Co are relatively thick as the same areas are generally devoid of Cu.

XRD results, shown in Fig. 9 did not reveal anything related to the new phase that was identified in SEM, as the new phase was only identified in experiment A5, of which not enough residue remained for XRD. In the selected samples (A6 and A9), XRD did confirm presence of delithiated $Li_{0.51}CoO_2$ in samples from Cu-Fe-H_2SO_4 leaching system. Sample A3 was from Fe-H_2SO_4 system, and delithiation in the residue had progressed further, hence the presence of $Li_{0.35}CoO_2$. The last remaining unidentified peaks were identified by calculation as K_β radiation as no optical monochromator, but only iron beta filter, was used in the analysis setup. The largest signals were in excess of 300 k counts, explaining the ease at K_β was observed. $LiCoO_2 > 99.5\%$ is the original commercial raw material that was used in the experiments, characterized prior to leaching. A few peaks that could be associated with Co_3O_4

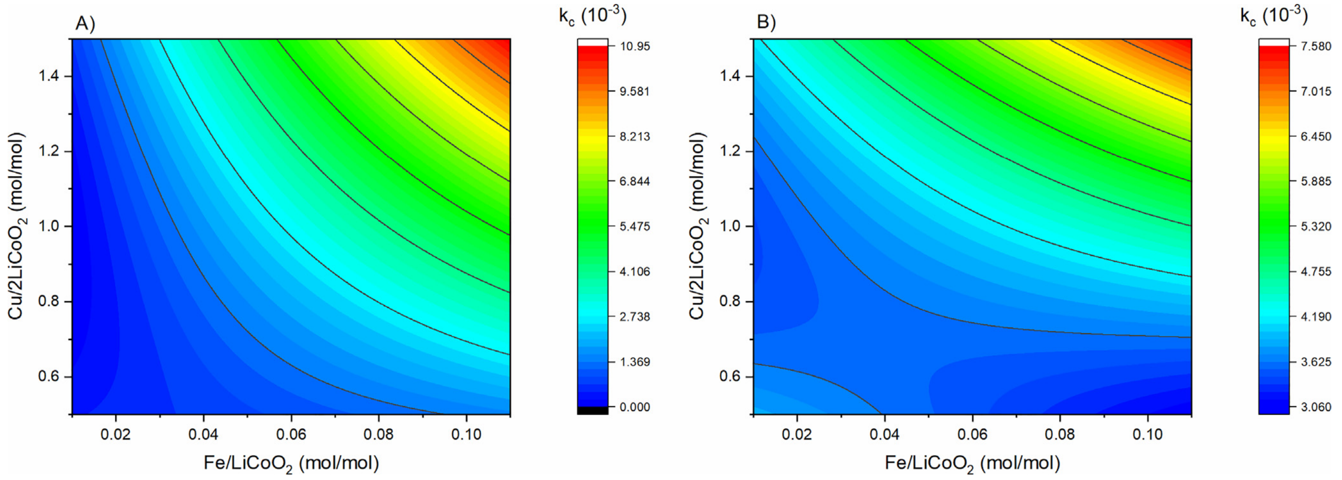

Fig. 6. Contour plot of the Model 2 (Fig. 7A) for predicting the reaction rate constant past the 30 min point, $1-(1-x)^{1/3} = k_c t$. Model 1 is presented in Fig. 7B, showing that the source of noise is the lower part ($k_c < 3.625$).

Table 6
Fe contents in samples with either low dissolution efficiency (A7, A9), with highest (A8) and mediocre (A12).

t (min)	A6 (mg/L)	A7 (mg/L)	A8 (mg/L)	A9 (mg/L)	A10 (mg/L)	A11 (mg/L)	A12 (mg/L)	A13 (mg/L)	A14 (mg/L)	A15 (mg/L)	A16 (mg/L)
5	97	99	1116	603	556	545	1153	562	1017	96	551
10	95	97	1096	590	537	544	1127	567	1008	94	574
15	94	96	1087	584	504	546	1136	554	1025	94	607
30	92	95	1112	578	511	535	1156	551	985	104	585
60	90	96	1115	572	527	525	1128	552	992	105	565
120	89	93	1113	570	527	519	1102	549	998	101	574

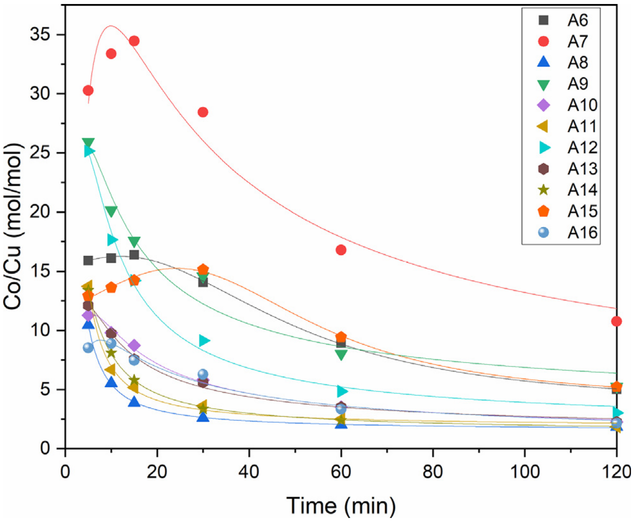

Fig. 7. The mol/mol of dissolved Co^{2+} vs. Cu^{2+} respectively.

was also obtained akin to results of Takacova et al. [31].

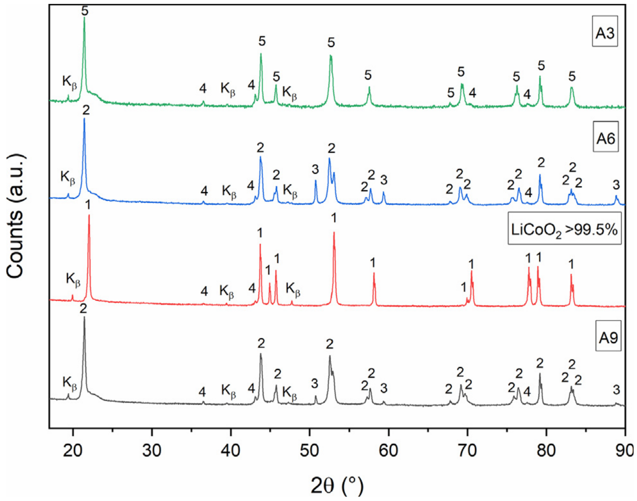

Fig. 9. XRD diffractograms of the LR of A6, original raw material ($LiCoO_2$, purity > 99.5% and A9, showing peaks of 1: $LiCoO_2$ (ICDD: 98-017-2909), 2: $Li_{0.51}CoO_2$ (ICDD: 98-016-0719), 3: Cu (ICDD: 98-005-3757), 4: Co_3O_4 (ICDD: 98-002-7504) and 5: $Li_{0.35}CoO_2$ (ICDD: 98-017-2912). The counts were logarithmically scaled.

3.5. Application on hydrometallurgical recycling

Based on the obtained results, it is possible to dissolve the LIB active material phases such as $LiCoO_2$ and its derivatives by applying Cu and Fe instead of using the widely investigated H_2O_2 in reduction. However, this method would bring its own challenges, such as simultaneous, high dissolution of Cu and Fe. The experiments performed here show that obtaining a solution with 10 g/L of Co, originating from $LiCoO_2$ with leaching efficiency of > 95%, will require 1.06 g/L of Fe as a catalyst,

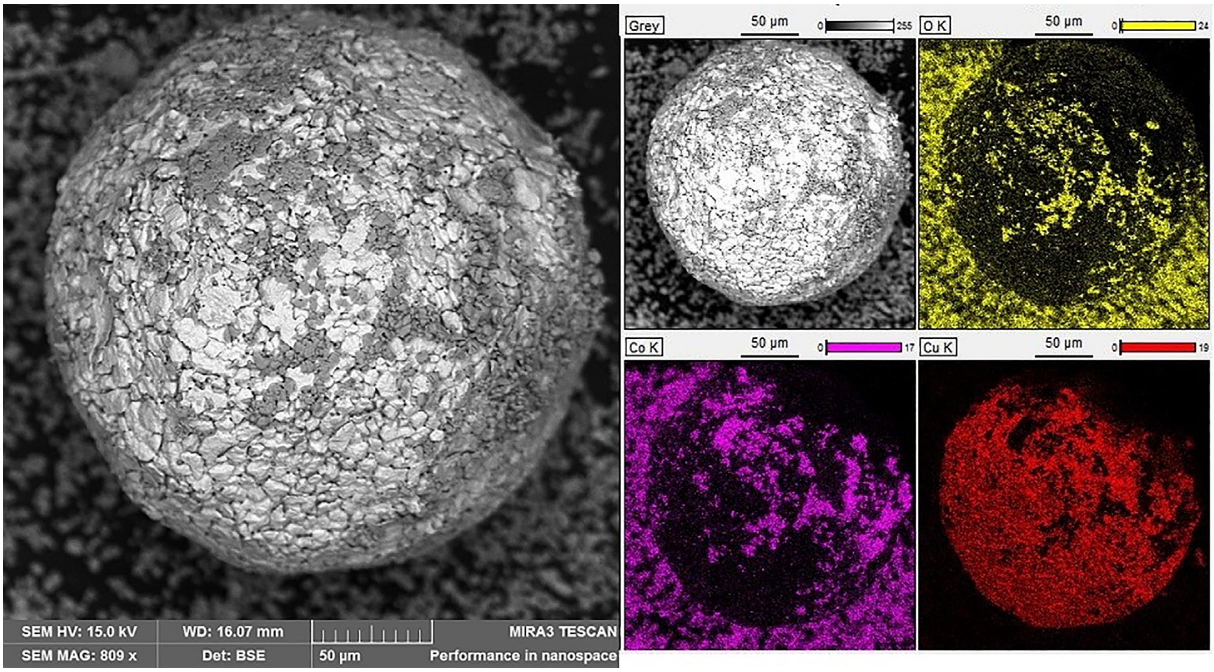

Fig. 8. SEM-EDX semi-quantitative mapping results of a copper particle, embedded with $LiCoO_2$ (A10).

and at least 2.167 g of Cu per 6.68 g of $LiCoO_2$, equaling to *Cu/2LiCoO₂* = 1/1 mol/mol ratio (exp. A14). Not all of the Cu dissolved however, and the undissolved portion could be filtered off and used in a next cycle. A typical LIB pack in EV contains 14.8 wt% of active oxide materials [32]. This suggests that with a similar ratio, 4.8 wt% Cu (per battery pack) is required to dissolve the active oxides present i.e. 4.8 g of Cu per 100 g of battery pack, crushed for recycling. A typical battery pack contains 9.1 wt% of Cu as a current collector material in anode. Therefore, the amount of copper present in battery pack is suggested to be sufficient for being used as the reductant for the leaching of the active oxides present in a waste battery mass. If a recycling process is to implement a Cu recovery circuit, it could be possible to utilize Cu from current collectors as a reductant for $LiCoO_2$ in an iron catalyzed H_2SO_4 leaching system. As a catalyst, the required quantity of Fe remains relatively low, and would need to be removed in the recovery and purification stages. This suggests that the separation of copper vs. black mass is not a necessity, but rather an opportunity for an efficient hydrometallurgical battery recycling process. Any sufficient amount of dissolved Fe present in the solution can be turned into advantage in the leaching system that is trying to ensure the dissolution of Cu and active materials.

4. Conclusions

In this study, the effect of metallic Cu and dissolved Fe on the dissolution kinetics of $LiCoO_2$ were investigated. It was shown that ferrous iron is able to reduce $LiCoO_2$, achieving > 95% Co extraction. It was also determined that Cu dissolution is enhanced in presence of $LiCoO_2$, but not through galvanic interactions.

Reaction kinetics were investigated at $T = 30\,^\circ C$ in 2 M H_2SO_4. Parameters were $Cu/2LiCoO_2 = 0.5\text{–}1.5$ mol/mol and $Fe/LiCoO_2 = 0.01\text{–}0.11$ mol/mol. It was found that the rate-limiting step in $LiCoO_2$ dissolution by catalytic total reaction (21) was related to Fe(II)/Fe(III) redox pair and metallic Cu. The reaction rate results conformed to cubic rate law, indicating that a reaction-controlled shrinking core model was applicable. The resultant reaction rate constants were analyzed with design of experiments, highlighting the potential use of DOE as a supporting tool in the analysis of reaction rate constants and their relation to reaction mechanism. Strong interaction of *[Fe]* and *[Cu]* was detected, meaning that the proposed catalytic reaction was occurring as expected per the reaction (21). The response surface model revealed that at the investigated parameter level, the reaction rates improve as if the Co dissolution is affected by the binomial term of $[Cu]^2$ after 30 min (confidence level 90%). This indicates that Cu may have weak galvanic interactions with $LiCoO_2$. Regression models were fitted, providing a tool for estimating the rate constant of dissolution reaction for future comparisons with real recycled battery active materials.

In the characterization of leach residues, a new, unreported phase was identified, however accurate characterization remained elusive. Indirect evidence points towards insoluble sulfate precipitates that were resistant towards water washing.

Finally, it is concluded that it was possible to obtain good Co extractions at low temperature of 30 °C, without any H_2O_2 addition, with a system containing 1.06 g/L Fe (19 mM) as a catalyst, and 2.167 g of Cu per 6.68 g of $LiCoO_2$, equaling to 1/1 mol ratio of $Cu/2LiCoO_2$. Ferrous ions are able to reduce Co in $LiCoO_2$, and the produced ferric ion is able to oxidize in turn metallic Cu present in sulfuric acid solution. Based on literature data on typical LIB cell, this Cu requirement could be fulfilled by the supply of recycled batteries. The amount of Fe required for the reaction to proceed is low and can be supplied by either the waste itself or as an additional reagent.

Declaration of Competing Interest

The authors declare that they have no known competing financial interests or personal relationships that could have appeared to influence the work reported in this paper.

Acknowledgements

For funding this research, the authors would like to acknowledge BATCircle (grant number 4853/31/2018), funded by Business Finland. This work made use of RawMatTERS Finland Infrastructure (RAMI) funded by Academy of Finland.

References

[1] A. Chagnes, J. Swiatowska, Lithium Process Chemistry: Resources, Extraction Batteries, and Recycling, Elsevier Science, 2015.

[2] C. Peng, J. Hamuyuni, B.P. Wilson, M. Lundström, Selective reductive leaching of cobalt and lithium from industrially crushed waste Li-ion batteries in sulfuric acid system, Waste Manage. 76 (2018) 582, https://doi.org/10.1016/j.wasman.2018.02.052.

[3] A. Porvali, M. Aaltonen, S. Ojanen, O. Velazquez-Martinez, E. Eronen, F. Liu, B.P. Wilson, R. Serna-Guerrero, M. Lundström, Mechanical and hydrometallurgical processes in HCl media for the recycling of valuable metals from Li-ion battery waste, Resour. Conserv. Recy. 142 (2019) 257–266, https://doi.org/10.1016/j.resconrec.2018.11.023.

[4] M.A. Hannan, M.S.H. Lipu, A. Hussain, A. Mohamed, A review of lithium-ion battery state of charge estimation and management system in electric vehicle applications: challenges and recommendations, Renew. Sust. Energ. Rev. 78 (2017) 834–854, https://doi.org/10.1016/j.rser.2017.05.001.

[5] T. Tirronen, D. Sukhomlinov, H. O'Brien, P. Taskinen, M. Lundström, Distributions of lithium-ion and nickel-metal hydride battery elements in copper converting, J. Clean. Prod. 168 (2017) 399–409, https://doi.org/10.1016/j.jclepro.2017.09.051.

[6] Y. Guo, F. Li, H. Zhu, G. Li, J. Huang, W. He, Leaching lithium from the anode electrode materials of spent lithium-ion batteries by hydrochloric acid (HCl), Waste Manage. 51 (2016) 227–233, https://doi.org/10.1016/j.wasman.2015.11.036.

[7] D. Dutta, A. Kumari, R. Panda, S. Jha, D. Gupta, S. Goel, M.K. Jha, Close loop separation process for the recovery of Co, Cu, Mn, Fe and Li from spent lithium-ion batteries, Sep. Purif. Technol. 200 (2018) 327–334, https://doi.org/10.1016/j.seppur.2018.02.022.

[8] L. Chen, X. Tang, Y. Zhang, L. Li, Z. Zeng, Y. Zhang, Process for the recovery of cobalt oxalate from spent lithium-ion batteries, Hydrometallurgy 108 (2011) 80–86, https://doi.org/10.1016/j.hydromet.2011.02.010.

[9] X. Chen, B. Xu, T. Zhou, D. Liu, H. Hu, S. Fan, Separation and recovery of metal values from leaching liquor of mixed-type of spent lithium-ion batteries, Sep. Purif. Technol. 144 (2015) 197–205.

[10] F. Liu, C. Peng, A. Porvali, Z. Wang, B.P. Wilson, M. Lundström, Synergistic recovery of valuable metals from spent nickel-metal hydride batteries and lithium-ion batteries, ACS Sustain. Chem. Eng. (2019), https://doi.org/10.1021/acssuschemeng.9b02863.

[11] W. Lv, Z. Wang, H. Cao, Y. Sun, Y. Zhang, Z. Sun, A critical review and analysis on the recycling of spent lithium-ion batteries, ACS Sustain. Chem. Eng. 6 (2018) 1504–1521, https://doi.org/10.1021/acssuschemeng.7b03811.

[12] J. Nan, D. Han, X. Zuo, Recovery of metal values from spent lithium-ion batteries with chemical deposition and solvent extraction, J. Power Sources 152 (2005) 278–284, https://doi.org/10.1016/j.jpowsour.2005.03.134.

[13] D.A. Ferreira, L.M.Z. Prados, D. Majuste, M.B. Mansur, Hydrometallurgical separation of aluminium, cobalt, copper and lithium from spent Li-ion batteries, J. Power Sources 187 (2009) 238–246, https://doi.org/10.1016/j.jpowsour.2008.10.077.

[14] J.M. Fernández-Rodríguez, L. Hernán, J. Morales, J.L. Tirado, Low-temperature hydrothermal transformations of LiCoO2 and HCoO2, Mater. Res. Bull. 23 (1988) 899–904, https://doi.org/10.1016/0025-5408(88)90084-0.

[15] G. Dorella, M.B. Mansur, A study of the separation of cobalt from spent Li-ion battery residues, J. Power Sources 170 (2007) 210–215, https://doi.org/10.1016/j.jpowsour.2007.04.025.

[16] P. Meshram, B.D. Pandey, T.R. Mankhand, Recovery of valuable metals from cathodic active material of spent lithium ion batteries: leaching and kinetic aspects, Waste Manage. 45 (2015) 306–313, https://doi.org/10.1016/j.wasman.2015.05.027.

[17] M. Joulié, E. Billy, R. Laucournet, D. Meyer, Current collectors as reducing agent to dissolve active materials of positive electrodes from Li-ion battery wastes, Hydrometallurgy 169 (2017) 426–432, https://doi.org/10.1016/j.hydromet.2017.02.010.

[18] C. Peng, F. Liu, A.T. Aji, B.P. Wilson, M. Lundström, Extraction of Li and Co from industrially produced Li-ion battery waste – Using the reductive power of waste itself, Waste Manage. 95 (2019) 604–611, https://doi.org/10.1016/j.wasman.2019.06.048.

[19] Outotec, HSC Chemistry, https://www.outotec.com/products/digital-solutions/hsc-chemistry/9.4.1 (2018).

[20] M. Muruganandham, R.P.S. Suri, Sh. Jafari, M. Sillanpää, J.J.Wu. Gang-Juan Lee, M. Swaminathan, Recent developments in homogeneous advanced oxidation processes for water and wastewater treatment, Int. J. Photoenergy. 21 (2014) 821674, https://doi.org/10.1155/2014/821674.

[21] H. Fritz, W. Joseph, W.J. Pope, The catalytic decomposition of hydrogen peroxide by iron salts, Proc. R. Soc. Lon. Ser-A. 147 (1934) 332–351, https://doi.org/10.

1098/rspa.1934.0221.
[22] C. Hanisch, W. Haselrieder, A. Kwade, Method for reclaiming active material from a galvanic cell, and an active material separation installation, particularly an active metal separation installation. U.S. Patent 9,780,419 (2017).
[23] J. Pudas, A. Erkkila, J. Viljamaa, Battery recycling method. U.S. Patent No. 8,979, 006 (2015).
[24] J.M. Casas, F. Alvarez, L. Cifuentes, Aqueous speciation of sulfuric acid–cupric sulfate solutions, Chem. Eng. Sci. 55 (2000) 6223–6234, https://doi.org/10.1016/S0009-2509(00)00421-8.
[25] J.M. Casas, G. Crisóstomo, L. Cifuentes, Dissolution of metallic copper in aqueous sulphuric acid - ferric sulphate solutions, Can. Metall. Q. 45 (2006) 243–248, https://doi.org/10.1179/cmq.2006.45.3.243.
[26] D. Mishra, D. Kim, D.E. Ralph, J. Ahn, Y. Rhee, Bioleaching of metals from spent lithium ion secondary batteries using Acidithiobacillus ferrooxidans, Waste Manage. 28 (2008) 333–338, https://doi.org/10.1016/j.wasman.2007.01.010.
[27] M.A. Bezerra, R.E. Santelli, E.P. Oliveira, L.S. Villar, L.A. Escaleira, Response surface methodology (RSM) as a tool for optimization in analytical chemistry, Talanta. 76 (2008) 965–977, https://doi.org/10.1016/j.talanta.2008.05.019.
[28] Minitab Inc., Minitab 17.1. (https://www.minitab.com).
[29] E. Billy, M. Joulié, R. Laucournet, A. Boulineau, E. De Vito, D. Meyer, Dissolution mechanisms of LiNi1/3Mn1/3Co1/3O2 positive electrode material from lithium-ion batteries in acid solution, ACS Appl. Mater. Inter. 10 (2018) 16424–16435.
[30] M.L. Free, Hydrometallurgy: Fundamentals and Applications, John Wiley & Sons, Incorporated, Somerset, 2013.
[31] Z. Takacova, T. Havlik, F. Kukurugya, D. Orac, Cobalt and lithium recovery from active mass of spent Li-ion batteries: theoretical and experimental approach, Hydrometallurgy 163 (2016) 9–17, https://doi.org/10.1016/j.hydromet.2016.03.007.
[32] J. Diekmann, C. Hanisch, L. Froböse, G. Schälicke, T. Loellhoeffel, A. Fölster, A. Kwade, Ecological recycling of lithium-ion batteries from electric vehicles with focus on mechanical processes, J. Electrochem. Soc. 164 (2017) A6184–A6191, https://doi.org/10.1149/2.0271701jes.